New Phytologist

Research

LTP2 hypomorphs show genotype-by-environment interaction in early seedling traits in *Arabidopsis thaliana*

Cristina M. Alexandre[1], Kerry L. Bubb[1], Karla M. Schultz[1], Janne Lempe[2], Josh T. Cuperus[1] and Christine Queitsch[1,3]

[1]Department of Genome Sciences, University of Washington, Seattle, WA 98195, USA; [2]Julius Kühn Institute (JKI) – Federal Research Centre for Cultivated Plants, Institute for Breeding Research on Fruit Crops, Dresden, 1099, Germany; [3]Brotman Baty Institute for Precision Medicine, Seattle, WA 98195, USA

Authors for correspondence:
Josh T. Cuperus
Email: cuperusj@uw.edu

Christine Queitsch
Email: queitsch@uw.edu

Received: *5 June 2023*
Accepted: *26 September 2023*

New Phytologist (2024) **241:** 253–266
doi: 10.1111/nph.19334

Key words: cuticle integrity, gene-by-environment interaction, hypocotyl, hypomorph, lipid transfer protein, *LTP2*, nongenetic variation, phenotypic variation.

Summary

- Isogenic individuals can display seemingly stochastic phenotypic differences, limiting the accuracy of genotype-to-phenotype predictions. The extent of this phenotypic variation depends in part on genetic background, raising questions about the genes involved in controlling stochastic phenotypic variation.
- Focusing on early seedling traits in *Arabidopsis thaliana*, we found that hypomorphs of the cuticle-related gene *LIPID TRANSFER PROTEIN 2* (*LTP2*) greatly increased variation in seedling phenotypes, including hypocotyl length, gravitropism and cuticle permeability. Many *ltp2* hypocotyls were significantly shorter than wild-type hypocotyls while others resembled the wild-type.
- Differences in epidermal properties and gene expression between *ltp2* seedlings with long and short hypocotyls suggest a loss of cuticle integrity as the primary determinant of the observed phenotypic variation. We identified environmental conditions that reveal or mask the increased variation in *ltp2* hypomorphs and found that increased expression of its closest paralog *LTP1* is necessary for *ltp2* phenotypes.
- Our results illustrate how decreased expression of a single gene can generate starkly increased phenotypic variation in isogenic individuals in response to an environmental challenge.

Introduction

Genetically identical individuals can develop different phenotypes. Understanding the mechanistic underpinnings of this nongenetic phenotypic variation and the relative contributions of environmental factors and stochasticity holds promise for more accurate genotype–phenotype predictions. As early as 1920, Sewall Wright wrote that a sizable fraction of the environmental contribution to phenotypic variation is likely missed experimentally and suggested that stochasticity may play an important role in shaping individual phenotypes (Wright, 1920). Individuals sampled from an isogenic population can differ because of (1) stochastic differences in gene expression (Elowitz *et al.*, 2002; Blake *et al.*, 2003; Raser & O'Shea, 2004; Lomvardas *et al.*, 2006; Volfson *et al.*, 2006; Gimelbrant *et al.*, 2007), protein levels (Feinerman *et al.*, 2008) or metabolic states (Smith *et al.*, 2007; Heerden *et al.*, 2014); (2) parental effects (Perez *et al.*, 2017); or (3) differences in microenvironments, relative position or other contextual information (Eagle & Levine, 1967; Snijder *et al.*, 2009). None of these possible causes are mutually exclusive. Even subtle differences can have large cumulative effects, because the internal state of individuals affects how they respond to environmental factors. A classic example of environmentally induced heterogeneity is the behavior of a collection of temperature-sensitive cell cycle mutants in yeast. When grown asynchronously, these mutants show heterogeneous, nonheritable phenotypes due to individual cells experiencing the restrictive temperature treatment at different stages in the cell cycle (Hartwell *et al.*, 1974). A multitude of studies in animals and plants have shown that the extent of nongenetic phenotypic variation across individuals and populations depends in part on genotype, with some genetic backgrounds of the same species showing greater nongenetic variation (or less phenotypic robustness) than others (Waddington, 1942; Whitlock & Fowler, 1999; Ros *et al.*, 2004; Hall *et al.*, 2007; Hill *et al.*, 2007; Ansel *et al.*, 2008; Sangster *et al.*, 2008; Shen *et al.*, 2012; Ayroles *et al.*, 2015; Katsanos *et al.*, 2017).

The more that increased, nongenetic phenotypic variation occurs in a particular genetic background, the lower will be our ability to predict phenotype from genotype, because the same genetic variants will show different expressivity in different individuals (Queitsch *et al.*, 2002; Eldar *et al.*, 2009; Raj *et al.*, 2010; Burga *et al.*, 2011; Casanueva *et al.*, 2012; Lachowiec *et al.*, 2016; Zabinsky *et al.*, 2019). Therefore, nongenetic phenotypic variation has wide-ranging implications, from cancer drug resistance (Sharma *et al.*, 2010; Shaffer *et al.*, 2017; Márquez-Jurado

et al., 2018; Emert *et al.*, 2021) to microbial bioproduction (Delvigne & Goffin, 2014; Xiao *et al.*, 2016). In agriculture, trait uniformity is particularly highly prized (Finch-Savage & Bassel, 2016; Tran *et al.*, 2017) and breeding programs rely on parental performance. A better understanding of the genetic underpinnings of nongenetic phenotypic variation and their interplay with environmental factors might inform targeted breeding of more robustly performing varieties. In plants, several genes have been identified that affect nongenetic variation of traits like growth (Joseph *et al.*, 2015; Illouz-Eliaz *et al.*, 2019), organ size or number (Hall *et al.*, 2007; Hong *et al.*, 2016), germination (Abley *et al.*, 2021), early seedling phenotypes (Queitsch *et al.*, 2002; Mason *et al.*, 2016; Lachowiec *et al.*, 2018; Lemus *et al.*, 2023) and defense metabolites (Jimenez-Gomez *et al.*, 2011; Joseph *et al.*, 2015).

Here, we focus on hypocotyl elongation in the dark, an adaptive trait relevant to seedling establishment. Hypocotyl elongation in the dark shows large nongenetic variation in *Arabidopsis thaliana* (*c.* 10% coefficient of variation in hypocotyl length; Maloof *et al.*, 2001; Borevitz *et al.*, 2002; Queitsch *et al.*, 2002; Sangster *et al.*, 2008; Lachowiec *et al.*, 2018). We found that hypomorphs of *LTP2* (*LIPID TRANSFER PROTEIN 2*/AT2G38530), a highly expressed gene in dark-grown seedlings, show increased phenotypic variation under specific environmental conditions. Plant lipid transfer proteins (LTPs) are a family of small (*c.* 9 kDa) lipid-binding, cysteine-rich proteins that are commonly found in the shoot epidermis (Kader, 1996; Yeats & Rose, 2008). While structurally similar, LTPs have different expression patterns, suggesting functional specialization (Arondel *et al.*, 2000; Chae *et al.*, 2010). Lipid transfer proteins have been associated with antimicrobial activity and cuticle physiology and are implicated in a wide variety of biological processes (Molina & García-Olmedo, 1993; Buhot *et al.*, 2001; Maldonado *et al.*, 2002; Nieuwland *et al.*, 2005; Cameron *et al.*, 2006; Chae *et al.*, 2009; Debono *et al.*, 2009; Potocka *et al.*, 2012; Finkina *et al.*, 2016; Gao *et al.*, 2016).

LIPID TRANSFER PROTEIN 2 is abundant in the epidermal cell wall of dark-grown hypocotyls (Irshad *et al.*, 2008; Jacq *et al.*, 2017), where it promotes cuticle integrity and desiccation tolerance (Jacq *et al.*, 2017). We found that under certain environmental conditions, *LTP2* is necessary for full hypocotyl elongation in the dark, and that a decrease in *LTP2* expression increases variation in hypocotyl length, gravitropism and cuticle permeability in isogenic seedlings. Differences in epidermal morphology and cuticle permeability between long and short *ltp2* hypocotyls and between growth conditions that promote or mask trait variation suggest that loss of cuticle integrity in *ltp2* hypocotyls is the main determinant of this background's increased nongenetic phenotypic variation.

Materials and Methods

Plant material

Arabidopsis thaliana (L.) Heynh., all lines are in the Col-0 background. *ltp2-1* is SALK_026257 (ABRC) described previously (Jacq *et al.*, 2017). *ltp2-1* plants homozygous for the T-DNA insertion (Chr2:16,128,007 SALK project) were confirmed by PCR analysis with primer pairs CA340 (Chr2:16,128,062) + CA103 (Chr2:16,128,340) and CA249 (Chr2:16,127,7702) + CA103 (primer sequences in Supporting Information Table S1). *ltp2-2* is line DT7-3 (Marjorie Matzke lab, Taipei, Taiwan) described previously (Kanno *et al.*, 2004) and contains a transgene insertion located upstream of *LTP2*, mapped in Kanno *et al.*, (2004). Approximate location is Chr2:16,128,261, determined by sequencing the PCR fragment CA340 + CA103. *ltp2-2* plants were confirmed homozygous for the transgene insertion by PCR genotyping with the same primers as *ltp2-1*. The *ltp1ltp2* double knockdown line was generated by *Agrobacterium*-mediated (GV3101) co-transformation of Col-0 plants with the helper plasmid pSOUP (CD3-1124, ABRC) and the plasmid CSHL_0103F2 (ABRC), containing an artificial microRNA against both *LTP2* and *LTP1*. T0 seeds were selected on 15 mg ml^{-1} phosphinotricin (PPT/BASTA); PPT-resistant T1 plants were then propagated on 25 mg ml^{-1} PPT; only generations T3 and above, homozygous for the transgene, were used in hypocotyl assays.

Hypocotyl assays

Hypocotyl and root length Unless otherwise stated, all seed batches were single-seed descent. Seeds were sterilized, resuspended in 0.1% (w/v) Bacto agar (BD, Diagnostics, Franklin Lakes, NJ, USA) and spotted in a well-spaced fashion onto square plates containing 1× Murashige & Skoog media (MS Basal Salt Mixture) pH 5.8, with 0.5 g l^{-1} MES (Sigma-Aldrich), 0.3% Phytagel (Sigma-Aldrich) and 1% sucrose (w/v). Plates were double-sealed with Micropore surgical tape (3M Center, St Paul, MN, USA) and stratified in the dark for 4 d at 4°C. After stratification, plates were exposed to 3 h of light, then placed in vertical racks, wrapped in aluminum foil and kept at 22°C in a Conviron chamber (50% RH; 16 h : 8 h, light : dark; *c.* 100 µmol m^{-2} s^{-1}) for 7 d. For certain experiments, the age and media composition varied as indicated elsewhere. Genotype placement was randomized across racks, and each genotype was distributed over multiple plates per experiment. At 7 d after stratification, plates were opened and imaged on a fixed stand. ImageJ was used to trace and measure hypocotyl and root length for every seedling. The hypocotyl was scored from the collet (hypocotyl : root transition zone) till the shoot apical meristem. Root length was used to infer late germination; outlier hypocotyls with < 5 mm (at 7 d) were removed from the analysis. Despite our best efforts, hypocotyl elongation proved highly sensitive to random environmental effects, and differences in a few millimeters in mean were not uncommon between replicates, even when controlling for seed batch.

Hypocotyl-negative gravitropism The angle between the shoot apical meristem and an imaginary vertical line, drawn starting at the base of the hypocotyl, was used to quantify the negative gravitropic response in dark-grown hypocotyls at 7 d poststratification. Data were expressed as deviations off vertical (in degrees), with vertical representing perfect negative gravitropism. Measurements were done on ImageJ, as described for hypocotyl length.

Hypocotyl epidermal imaging The epidermal surface of dark-grown hypocotyls was imaged at 7 d poststratification. Whole seedlings were placed directly on a glass slide and the hypocotyl imaged using a Zeiss Axioplan microscope at ×50 magnification.

Toluidine blue assay Toluidine blue assay protocol based on Tanaka *et al.* (2004) but with a lower concentration of dye to avoid saturation in *ltp2*. Whole dark-grown seedlings were immersed in an aqueous solution of 0.02% (w/v) toluidine blue (Sigma) for 2 min with gentle shaking, then washed 3× with distilled water and left in water until imaging. ImageJ was used to determine hypocotyl length and the fraction of the total length stained with toluidine blue.

Seed size

Matched datasets of seed size and hypocotyl length were obtained by imaging the same plate twice: (1) after stratification, when seeds were fully imbibed, and (2) after 7 d of growth in the dark. The position of the seed and the hypocotyl are the same in both pictures. Between 10 and 20 seeds were spotted per plate and several plates were employed per genotype. For imaging seeds, pictures were taken under a stereomicroscope, at ×5 magnification. Seed area was measured in ImageJ using > 8-bit > Threshold (auto) > Analyze Particles, with settings: area, 5000-infinity; circularity ≥ 0.7.

qRT-PCR

Seedling samples were either single individuals or pools of *c.* 30 individuals. Unless otherwise stated, only the shoot was harvested (including hypocotyl, cotyledons and shoot apical meristem). For roots, rosette leaves and flowers, all samples were pools; roots were excised from 7-d-old seedlings; rosette leaves; and flowers from mature plants. RNA was extracted from LN2-frozen material using TRIzol (Invitrogen) and DNase I treated. cDNA was synthesized from 250 to 500 mg of total RNA with the RevertAid First Strand cDNA Synthesis Kit (Thermo Scientific, Waltham, MA, USA). qRT-PCR was performed with LightCycler 480 SYBR Green I Master Mix (Roche). Relative gene expression was calculated as $2^{-(Ct\ target - Ct\ reference)}$, with either *AP2M*/AT5G46630, *UBC21*/AT5G25760 or *PP2A*/AT1G13320 as reference genes. Primers are listed in Table S1.

RNA-Seq data

Setup and sequencing For each replicate of Col-0 and *ltp2-1*, seven hypocotyl assays were set up in parallel, each containing 64–70 seedlings. At Day 7 after stratification, hypocotyl length was scored for each of the seven assays, and from each, only the shoots of the 10 most extreme seedlings at either tail of the distribution (bottom and top 15th percentile) were collected as 'short' and 'long' samples, respectively. Each sample contained a total of 70 shoots and corresponds to one replicate. The process was repeated to obtain a second biological replicate, in a total of eight samples (Col-L1, Col-L2, Col-S1, Col-S2, *ltp2*-L1, *ltp2*-L2, *ltp2*-S1 and *ltp2*-S2). RNA was extracted from all samples in parallel using the SV Promega Total RNA System followed by NaCl/EtOH precipitation. Generation of RNA-Seq libraries, multiplexing and sequencing was outsourced to Genewiz Inc. (South Plainfield, NJ, USA). Each library was sequenced on four lanes and two flowcells of an Illumina HiSeq2500 (San Diego, CA, USA) in a 1 × 50-bp SE format.

Pseudoalignment of reads and estimation of transcript abundance Pseudoalignment of reads and estimation of transcript abundance was done using Kallisto (Bray *et al.*, 2016). The Kallisto index was built with *Arabidopsis thaliana* TAIR10 cDNA models ftp://ftp.ensemblgenomes.org/pub/plants/release-50/fasta/arabidopsis_thaliana/cdna/Arabidopsis_thaliana.TAIR10.cdna.all.fa.gz. Transcript abundances were quantified with parameters –single -l 200 -s 20. Kallisto abundance files were parsed into R (v.3.6.1) using tximport(). The tx2gene file and the TxDb object used TAIR10 annotations ftp://ftp.arabidopsis.org/home/tair/Genes/TAIR10_genome_release/TAIR10_gff3/TAIR10_GFF3_genes_transposons.gff.

The output was a matrix of estimated counts with 26 923 rows (genes) and 8 columns (samples).

Differentially expressed genes After nonspecific filtering to remove all nonexpressed genes (zero counts across all samples; 2917 genes), and all genes which did not have at least one count in all samples (4023), a filtered matrix of 19 983 genes × 8 samples was converted to integers and used as input for DESeq2 (Love *et al.*, 2014), with parameters: condition = genotype × hypocotyl length, with two biological replicates per condition. Only genes with a $\log_2$FC ≥ 1 and adjusted *P*-value ≤ 0.01 were called as differentially expressed genes (DEGs). As high fold changes are more frequent in genes with low baseline expression, we specifically chose a less stringent fold-change cutoff to avoid discarding genes with very high expression like *LTP2*. Differentially expressed genes were obtained for four different pairwise comparisons: (1) Col-L vs Col-S, (2) Col-L vs *ltp2*-L, (3) Col-S vs ltp2-S and (4) *ltp2*-L vs *ltp2*-S (Tables S2–S5).

Principal component analysis prcomp() was applied to a transposed standardized matrix of $\log_{10}$(counts) with 19 983 rows × 8 columns.

Gene Ontology enrichments Gene Ontology (GO) enrichments were obtained with g:Profiler (Raudvere *et al.*, 2019) https://biit.cs.ut.ee/gprofiler/gost, with the input to DESeq2 (a list of 19 983 genes) as background. Significant GO terms were shortlisted if fold enrichment ≥ 2 and Bonferroni-corrected *P*-value < 0.05. Query genesets were (1) the list of 584 DEGs between *ltp2*-L and *ltp2*-S and (2) the list of 1164 DEGs unique to the comparison Col-S and *ltp2*-S.

Cuticle genes From the dataset in Li-Beisson *et al.* (2013), we selected only genes with annotated roles in cutin or wax biosynthesis and/or deposition (groups Cuticle Synthesis and Transport 1, Fatty Acid Elongation & Wax Biosynthesis and Fatty Acid

Synthesis). The curated list contained 224 genes (Table S6), of which 160 were present in our RNA-Seq dataset (Table S6), and 21 were differentially expressed between Col-0 and *ltp2* (union set between Col-L vs *ltp2*-L and Col-S vs *ltp2*-S, 1717 DEGs); the hypergeometric test indicates this is a modest overrepresentation ($P = 0.019$).

Protein sequence tree of PR-14/LTP Type I proteins

Protein sequences for PR-14/Type I LTP proteins (Arondel *et al.*, 2000) were retrieved from NCBI: NP_181388.1 LTP1, NP_181387.1 LTP2, NP_568905.1 LTP3, NP_568904.1 LTP4, NP_190728.1 LTP5, NP_187489.1 LTP6, NP_973466.1 LTP7, NP_179428.1 LTP8, NP_179135.2 LTP9, NP_195807.1 LTP10, NP_680758.3 LTP11, NP_190727.1 LTP12, NP_001078707.1 LTP13, NP_001078780.1 LTP14 and NP_192593.3 LTP15. Multiple sequence alignment was done with ClustalW in the msa package (Bodenhofer *et al.*, 2015) and the neighbor-joining tree with the ape package (Paradis *et al.*, 2004).

LTP1 and *LTP2* global expression pattern

We used the Digital Expression Explorer 2 repository (Ziemann *et al.*, 2019) https://dee2.io/ to retrieve uniformly processed RNA-Seq data from *A. thaliana*. We curated a dataset of 56 samples, spanning several organs, contexts and developmental stages (Table S7), and kept only genes with at least three counts in one sample out of the 56 (26 372 genes × 56 samples).

Results

Decreased *LTP2* expression increases nongenetic phenotypic variation in skotomorphogenesis

Young seedlings grown in the dark show common skotomorphogenic phenotypes with elongated hypocotyls, etiolated cotyledons and short roots (Gendreau *et al.*, 1997; Vandenbussche *et al.*, 2005). *LIPID TRANSFER PROTEIN 2* is among the most highly expressed genes in dark-grown shoots (99th percentile, Fig. S1A,B), suggesting that its function is required during skotomorphogenesis. To measure the impact of *LTP2* on the phenotypic variation of elongating hypocotyls, we used two *ltp2* hypomorphs, *ltp2-1* and *ltp2-2*, harboring T-DNA insertions < 500-bp upstream of the *LTP2* transcriptional start site (Fig. 1a). Both lines expressed < 25% of wild-type *LTP2* RNA levels in dark-grown shoots (Fig. 1b) and showed similar defects in skotomorphogenesis. When grown in the dark, *ltp2* hypocotyls were shorter (Fig. 1c,d) and more variable than wild-type (Col-0; Fig. 1c), in both length (Fig. 1e) and orientation (Fig. 1f). Hypocotyl lengths were almost twice as variable in *ltp2-1* as in Col-0 wild-type (merged coefficient of variation, CV, of 21% vs 13%), with *ltp2-2* being slightly less variable (merged CV 18%; Fig. 1e). The higher variation in the hypomorphs was not due to a bimodal distribution but to a continuous, wider distribution of hypocotyl lengths (Fig. 1d). An even larger difference was measured for hypocotyl orientation (CV 34–37% vs 10%; Fig. 1f), a proxy for reduced negative gravitropism. However, there was no substantial correlation between hypocotyl length and orientation of individual seedlings (Fig. S1C). Consistent with a nongenetic origin for this increased variation in hypocotyl length, the selfed offspring of *ltp2* parents with either long or short hypocotyls showed similar mean hypocotyl lengths (Fig. 1g). Other notable *ltp2* phenotypes included longer roots than hypocotyls, resulting in a smaller hypocotyl : root ratio per individual seedling than in Col-0 wild-type (Fig. 1h), and a tendency for open and expanded cotyledons (Fig. 1c arrowhead, Fig. 1i). Taken together, reduced levels of *LTP2* globally affect nongenetic variation in skotomorphogenesis.

ltp2 phenotypes show strong gene-by-environment interaction

Next, we explored internal and external factors that might be associated with the hypocotyl length of individual seedlings or modulate the extent of phenotypic variation in *ltp2* hypomorphs. We started by examining the influence of seed batch, seed germination and seed size on hypocotyl length. We found similar mean hypocotyl lengths (Fig. S2A) and similarly high coefficients of variation with different *ltp2* seed batches (Fig. 1e). There was no germination delay or increased heterogeneity in germination in the *ltp2* hypomorphs relative to Col-0 wild-type, as inferred from the correlation of hypocotyl and root length and its time-dependent drop in seedling development (Fig. S2B). Finally, hypocotyl length of individual seedlings was not substantially explained by seed size in either the *ltp2* hypomorphs or Col-0 wild-type (Fig. S2C).

We continued by examining the impact of the growth medium. In the dark, hypocotyls grow longer if provided with sucrose. However, the presence of sucrose also modifies hypocotyl and root growth kinetics (Kircher & Schopfer, 2012; Fig. S3A) and is associated with a decrease in the hypocotyl : root ratio compared with growth conditions without sucrose (Kircher & Schopfer, 2012; Fig. S3B). We reasoned that the presence of sucrose might affect variation in hypocotyl elongation. In our typical experimental setup, seedlings grow in vertical plates, with hypocotyls in direct contact with the medium, and sucrose-driven hypocotyl elongation depends on shoot uptake (Fig. S3C). A comparison between *ltp2* seedlings grown on MS media, MS + 1% sucrose or MS + 1% glucose revealed that *ltp2* phenotypes were strongly sucrose-dependent. Either removing sucrose or replacing it with glucose was sufficient to rescue all *ltp2* growth phenotypes, including differences in mean length and coefficient of variation (Fig. 2a,b), hypocotyl-negative gravitropism (Fig. 2c) and hypocotyl length : root length ratio (Fig. 2d). Therefore, *ltp2* hypocotyls can fully elongate under favorable conditions. Sucrose did not cause an increase in the coefficient of variation of hypocotyl length in wild-type Col-0, despite a noticeable increase in mean length in this condition (Fig. 2a,b).

We wondered whether the effects of sucrose on *ltp2* seedlings involved osmotic stress. To test this possibility, we added mannitol to the growth medium. Mannitol causes strong osmotic stress in *Arabidopsis* seedlings (Zwiewka *et al.*, 2015; Kalve

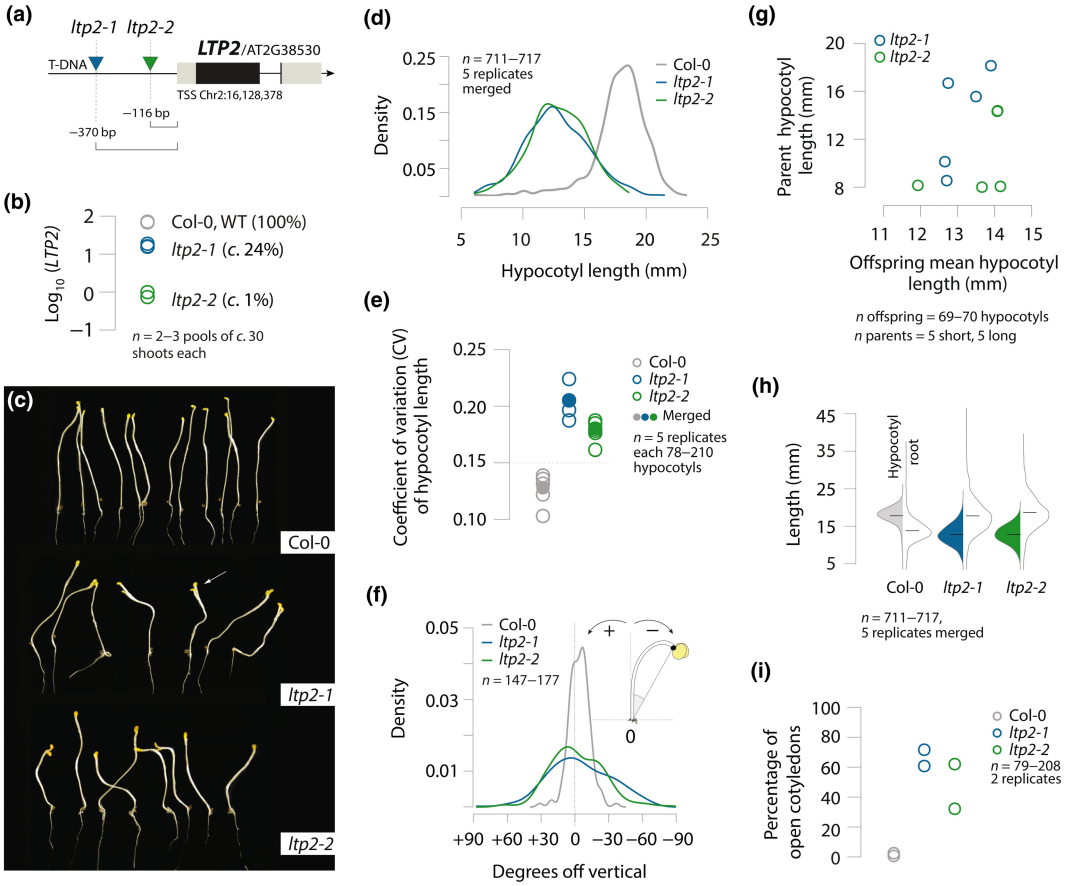

Fig. 1 *LIPID TRANSFER PROTEIN 2* (*LTP2*) hypomorphs increase phenotypic variation in skotomorphogenesis traits. (a) Approximate location of the T-DNA insertion (LB) relative to the *LTP2* gene in *ltp2-1* and *ltp2-2* lines. (b) *LTP2* relative expression in the shoots of wild-type (Col-0), *ltp2-1* and *ltp2-2* seedlings grown in the dark for 7 d after stratification. In parenthesis are the % of Col-0 *LTP2* transcript levels detected in the *ltp2* lines. (c) Representative image of Col-0 (top), *ltp2-1* (middle) and *ltp2-2* (bottom) dark-grown seedlings at 7 d after stratification; the roots were trimmed. (d) Density lines of the distributions of hypocotyl length scored at 7 d poststratification in Col-0 and *ltp2* seedlings grown in Murashige & Skoog (MS) media with 1% sucrose; each line represents the merged distribution of five biological replicates ($n = 78$–210 each) per genotype. (e) Coefficient of variation (SD/mean) in hypocotyl length, a measure of variation, for (1) five biological replicates (open circles) and (2) merged for all five replicates (filled circle, same data as in d). (f) Hypocotyl-negative gravitropism measured as the deviation from vertical (in degrees) of the hypocotyl apex in 7 d dark-grown seedlings grown on MS + 1% sucrose. The density distribution of measured angles for all genotypes is plotted. (g) Comparison between the hypocotyl length of individual *ltp2* parents (five long and five short) and the mean hypocotyl length of their offspring; all lengths measured at 7 d poststratification on seedlings grown on MS + 1% sucrose. (h) Beanplots of hypocotyl (left side) and root (right side) length from the merged dataset used in (d, e). (i) Percentage of dark-grown seedlings with an open cotyledon phenotype, in wild-type (Col-0), *ltp2-1* and *ltp2-2* genotypes, at 7 d after stratification on MS + 1% sucrose. Two replicates are shown ($n = 79$–208).

et al., 2020). Adding equimolar amounts of mannitol (29 mM) and sucrose (1%) together improved, rather than aggravated, the *ltp2* phenotypic defects (Fig. S4). We also considered whether *ltp2* seedlings were deficient in sucrose uptake but concluded that this scenario is unlikely because of the following results: The hypocotyls of *ltp2* seedlings remain sucrose-sensitive and show similar sucrose-driven responses as those of wild-type (Fig. S5). Furthermore, doubling the amount of sucrose inhibited hypocotyl elongation to the same extent in *ltp2* and wild-type seedlings (Fig. S5D). Lastly, *ltp2* hypocotyls were shorter when grown on MS + 1% sucrose compared with MS alone (Fig. 2a), with a significant difference in mean values (*ltp2-1*: 3.03 mm 95% CI 2.62–345, *ltp2-2*: 3.96 mm 95% CI 3.54–4.38, *ltp2-1*: $t(258.75) = 14.459$; $P < 2.2e\text{-}16$, *ltp2-2*: $t(274.64) = 18.5$; $P < 2.2e\text{-}16$), inconsistent with deficient sucrose uptake. We conclude that neither osmotic stress nor sucrose uptake contribute substantially to the *ltp2* phenotypes.

A sucrose-dependent increase in cuticle permeability is associated with short *ltp2* hypocotyls

A comparison of *ltp2* hypocotyls grown with and without sucrose revealed epidermal features that were associated with short hypocotyls. Compared with wild-type Col-0, the epidermal surface of *ltp2* hypocotyls was not smooth and instead was fuzzy or wrinkled (Fig. 2e); this *ltp2* phenotype was sucrose-specific and much stronger in short than in long *ltp2* hypocotyls (Fig. 2e). Furthermore, growth with sucrose greatly increased permeability to the water-soluble dye toluidine blue, an indicator of cuticle integrity (Tanaka *et al.*, 2004), in *ltp2* hypocotyls, but not in Col-0 hypocotyls,

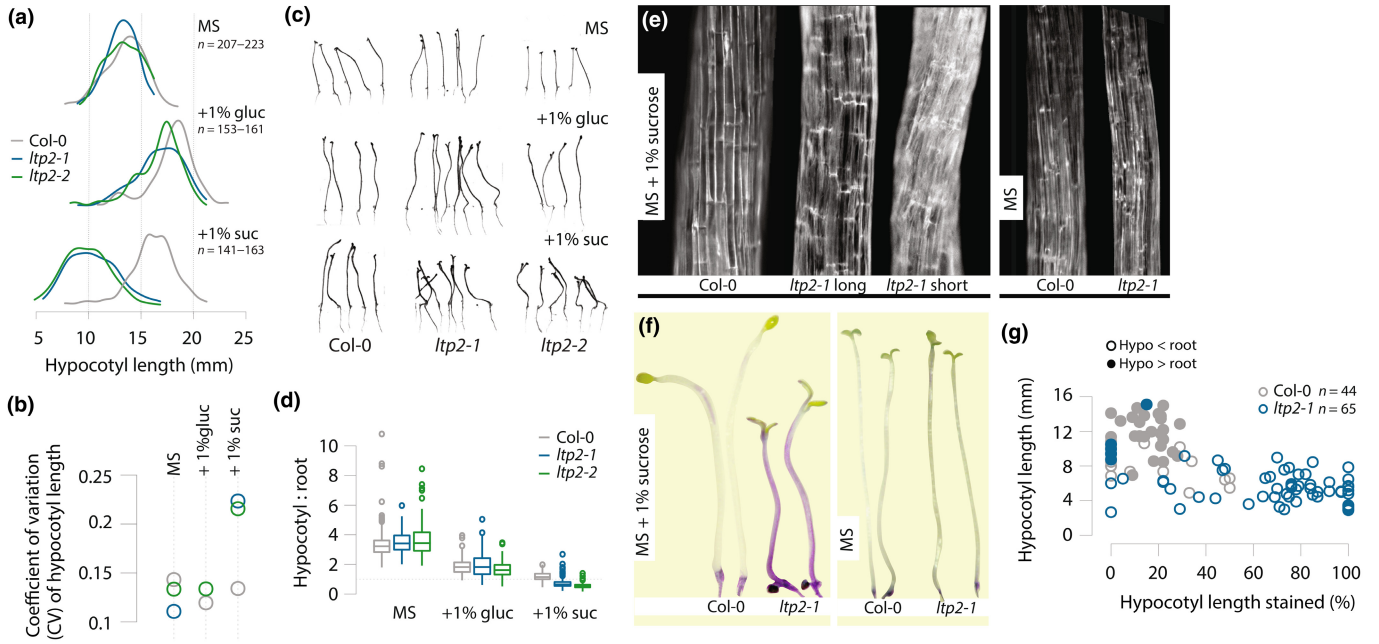

Fig. 2 Sucrose-dependent loss of cuticle integrity in *ltp2* is associated with short hypocotyls. (a) Density lines of the distribution of hypocotyl length for seedlings grown on plates containing Murashige & Skoog (MS) medium, MS + 1% glucose or MS + 1% sucrose for 7 d poststratification. Shown are the merged distributions of two biological replicates per condition/per genotype. (b) Coefficient of variation in hypocotyl length for the distributions shown in (a). (c) Representative shoots of 7 d dark-grown seedlings grown on plates containing MS medium, MS + 1% glucose or MS + 1% sucrose. Hypocotyl-negative gravitropism is largely rescued in *ltp2* seedlings grown without sucrose. (d) Boxplots comparing the hypocotyl : root ratio for every seedling in (a) across different growth media. Within each boxplot, horizontal lines denote median values; boxes extend from the 25th to 75th percentiles; veritcal lines represent values within 1.5 interquartile ranges of the 25th and 75th percentiles; circles are outside of these ranges. (e) Magnified images of the epidermal surface of Col-0 and *ltp2-1* hypocotyls at 7 d poststratification when grown with (left) or without (right) 1% sucrose. (f) Comparing the effects of 1% sucrose on hypocotyl cuticle permeability: dark-grown seedlings of Col-0 and *ltp2-1* were stained with toluidine blue after growing for 5 d on MS + 1% sucrose (left) or 7 d on MS alone (right). (g) Relationship between hypocotyl length at 7 d after stratification on MS + 1% sucrose and toluidine blue staining coverage expressed in % of hypocotyl length. Filled dots represent seedlings with the wild-type developmental pattern of hypocotyl length > root length.

compared with controls without sucrose. Most *ltp2* hypocotyls stained deeply, and over > 50% of their full length (Fig. 2f,g), consistent with reduced cuticle integrity (Jacq *et al.*, 2017). The extent of staining varied widely in *ltp2* hypocotyls, from 0% to 100% (Fig. 2g). On average, heavily stained hypocotyls were smaller than those not stained (Fig. 2g), and *ltp2* seedlings with the wild-type-like hypocotyl length : root length ratio > 1 were less stained overall (Fig. 2g). By contrast, staining in Col-0 wild-type hypocotyls was generally weak and spatially restricted (Fig. 2f,g). These results suggest that altered cuticle integrity contributes to the sucrose-dependent inhibition of hypocotyl elongation in *ltp2* seedlings.

Hypocotyl length is associated with many transcriptional differences in *ltp2* seedlings

To identify what molecular functions are associated with nongenetic variation in hypocotyl length, we compared the transcriptional profiles of Col-0 and *ltp2-1* seedlings with short (S) and long (L) hypocotyls (bottom and top 15th percentiles, respectively; Fig. 3a). For each genotype by length combination, we performed bulk RNA-Seq on two replicate pools of 70 shoots each (Fig. 3a, see Fig. S6A–C for QC metrics). Principal component analysis showed three clearly distinguishable clusters: one formed by Col-0 L and S samples, a second formed only by *ltp2-1* L samples and a third containing the *ltp2-1* S samples (Fig. 3b). Nearly half of the global variance in gene expression (47%, PC1) was correlated with mean hypocotyl length (Fig. 3c). Over 20 times as many DEGs ($\log_2$FC ≥ 1 and *P*-adj < 0.01) were found between the short and long *ltp2* samples (584, Table S3) compared with the Col-0 samples (24, Table S2). The DEGs associated with hypocotyl length in *ltp2* samples were enriched in GO terms related to cell wall modification, response to stress and plant defense (Fig. 3d, fold enrichment ≥ 2, *P*-adj < 0.05). *ltp2* samples with short hypocotyls showed downregulation of cell wall-related genes that promote growth, like *PGX1* and *XTH20* (Miedes *et al.*, 2013; Xiao *et al.*, 2014), secondary cell wall biosynthesis genes, including the three main laccases *LAC4*, *LAC11* and *LAC17*, and several peroxidases and genes related to Casparian strip deposition (Fig. 3e). Although Casparian strip biology is not well studied outside of roots, the Casparian strip is present in dark-grown hypocotyls (Karahara, 2012; Geldner, 2013). None of the genes in the enriched term 'Casparian strip' were differentially expressed between Col-0 wild-type and *ltp2* seedlings with long hypocotyls (Fig. 3e), suggesting that the downregulation of these genes may contribute to the phenotype of *ltp2* seedlings with short hypocotyls.

We also observed the upregulation of a variety of stress and defense-response genes related to hypoxia, response to fungus, anthocyanin and jasmonate biosynthesis (Fig. 3f). A few of these

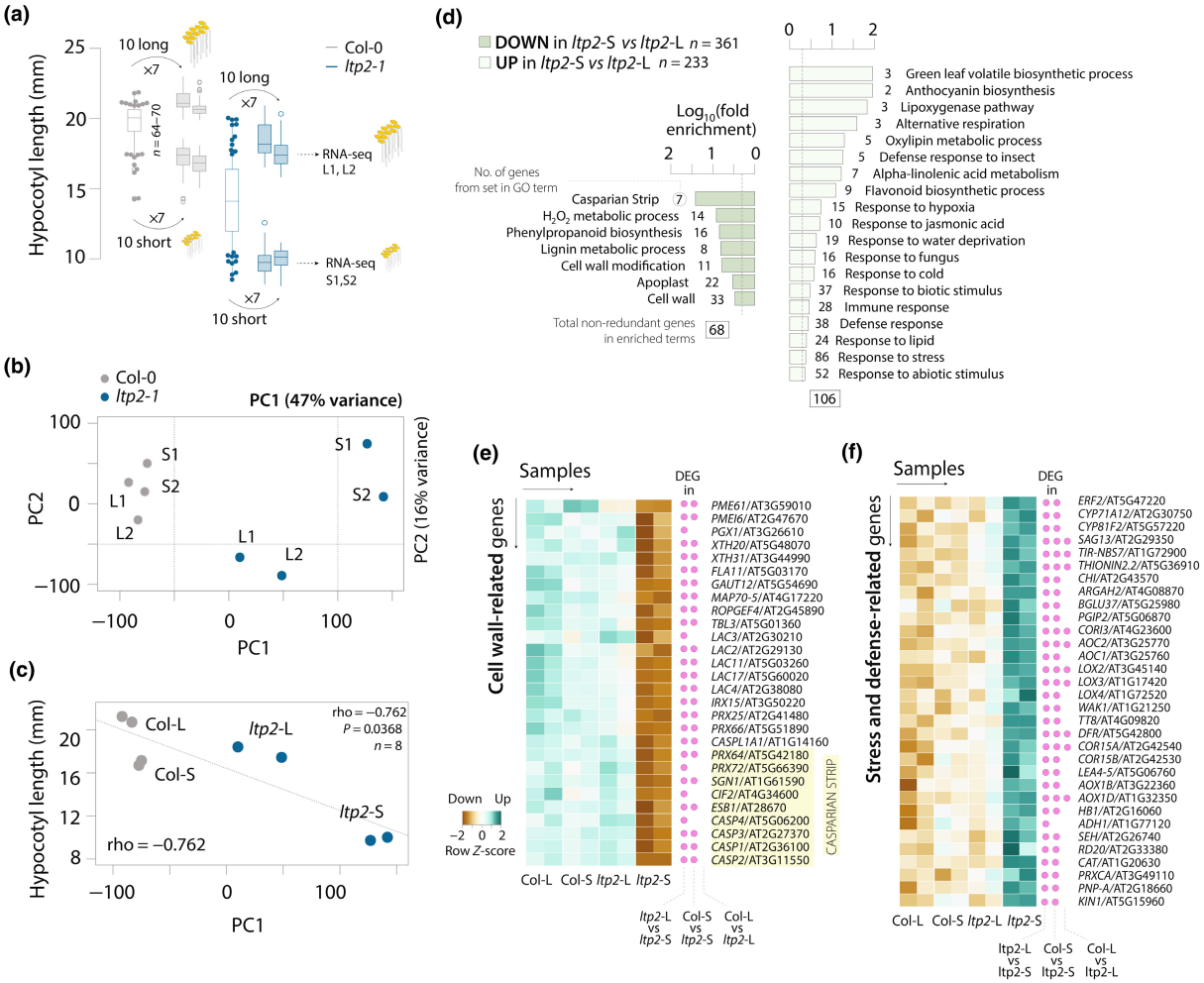

Fig. 3 Hypocotyl length is associated with many transcriptional differences in *ltp2* but not Col-0 seedlings, mostly related to stress, defense and growth. (a) Experimental setup for collecting RNA-Seq samples. For Col-0 and *ltp2-1*, the first boxplot shows the distribution of hypocotyl length from one out of seven hypocotyl assays done per replicate; the second set of four boxplots (two replicates with short and two replicates with long hypocotyls) shows the actual distribution of hypocotyl lengths ($n = 70$) from the selected individuals used to generate RNA-Seq libraries. Within each plot, horizontal lines denote median values; boxes extend from the 25th to 75th percentiles; vertical lines denote adjacent values within 1.5 interquartile ranges from the 25th to 75th percentiles; circles are observations outside of these ranges. (b) Biplot of principal component analysis showing the first two PCs. The percentage of the total variance explained by PC1 and PC2 is indicated on the top right corner. (c) Correlation between mean hypocotyl length for the eight RNA-Seq samples and PC1 loadings; shown on the bottom left corner is the Spearman rho. (d) Shortlisted Gene Ontology (GO) enrichments (fold enrichment ≥ 2 and adjusted *P*-value < 0.05) for the set of 584 differentially expressed genes (DEGs) between *ltp2*-L and *ltp2*-S, split by down- and upregulated genes. Shown are the $\log_{10}$(fold-enrichment) and the number of DEGs per enriched term. (e, f) Row-scaled heatmap visualizations of a subset of DEGs downregulated (e) or upregulated (f) in *ltp2*-S relative to *ltp2*-L. Pink dots indicate whether each gene was also a DEG on other pairwise comparisons.

genes (11), including several of the most highly upregulated genes in *ltp2* seedlings with short hypocotyls (Fig. S6E), were also upregulated in Col-0 seedlings with short hypocotyls compared with Col-0 seedlings with long hypocotyls (Fig. S6D). This result supports the idea that the phenotypic impact of perceived stress on hypocotyl length for a given individual can be genotype-independent; however, *ltp2* individuals experience this impact far more frequently and far more severely.

The majority of the DEGs (474, 81%) between the long and short *ltp2* samples were also differentially expressed between the short samples of *ltp2* and Col-0. This result likely reflects that the difference in mean hypocotyl length between the short *ltp2* and the short wild-type samples is about as large as the difference between the long and the short *ltp2* samples (Fig. S6F). However, we found more than twice as many DEGs (1638) in the comparison of the short *ltp2* and short wild-type samples (Fig. S6G). These DEGs showed similar GO enrichments as found for the comparison of long and short *ltp2* samples, related to hypoxia, oxidative stress, plant defense and cell wall metabolism, with additional growth-related terms such as response to auxin (Fig. S6H). Indeed, we found that many auxin-responsive genes, including some with known roles in hypocotyl elongation and/or gravitropism like *SAUR19/23/24/32* (Park *et al.*, 2007; Spartz *et al.*, 2012), *ARGOS* (Rai *et al.*, 2015), *SHY2* (Reed *et al.*, 1998; Tian *et al.*, 2002) and *HAT2* (Sawa *et al.*, 2002), were downregulated in *ltp2* seedlings with short hypocotyls compared with wild-type seedlings with short hypocotyls, but not compared with *ltp2* seedlings with long hypocotyls (Table S8). Most of the DEGs in

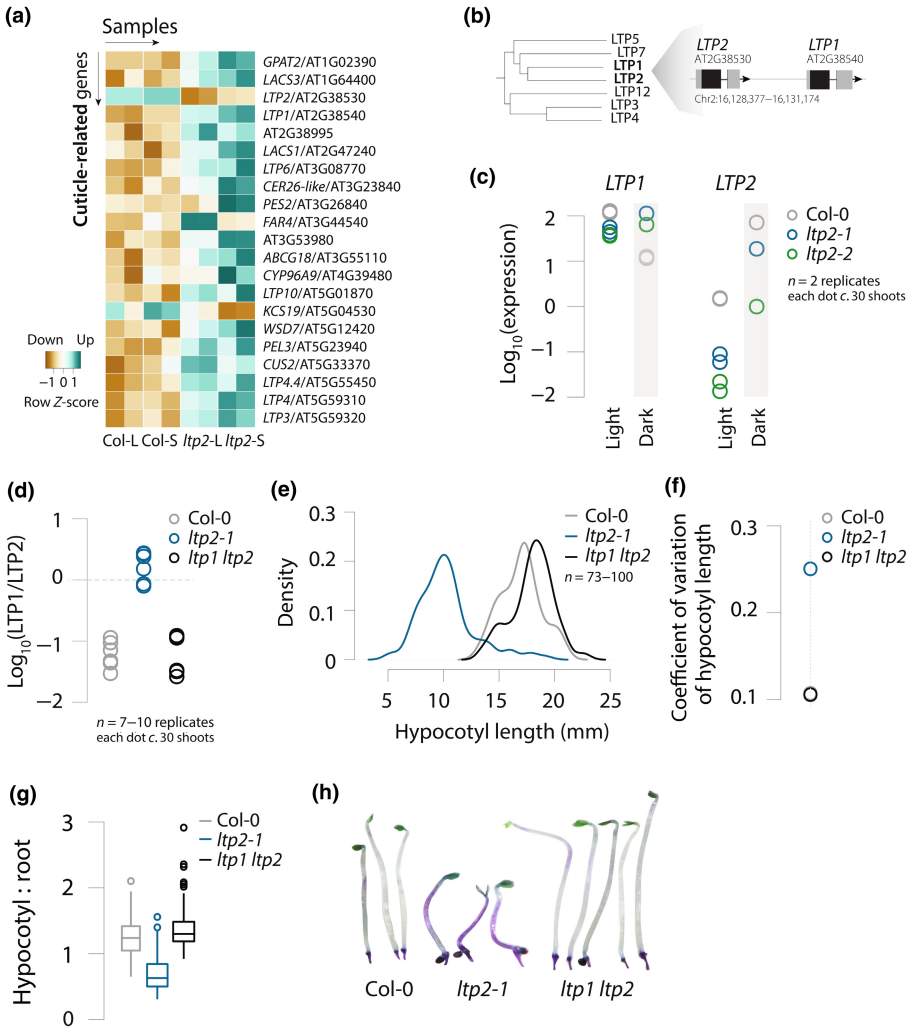

Fig. 4 *ltp2* phenotype depends on the expression ratio of *LIPID TRANSFER PROTEIN 2* (*LTP2*) and its close paralog *LTP1*. (a) Row-scaled heatmap visualization of cuticle-related genes differentially expressed between Col-0 and *ltp2* samples. (b) Detail of a tree depicting amino acid sequence similarity among PR14/Type I LTP proteins (full tree in Supporting Information Fig. S5A). (c) Relative expression of *LTP1* and *LTP2* in the shoots of light or dark-grown (gray box) Col-0 and *ltp2* seedlings grown for 7 d after stratification on Murashige & Skoog (MS) media + 1% sucrose. (d) Comparison of the *LTP1*/*LTP2* expression ratio between Col-0, *ltp2-1* and an *ltp1ltp2* double mutant. (e, g) Hypocotyl length distribution (e), coefficient of variation of hypocotyl length (f) and (g) hypocotyl : root ratio for Col-0, *ltp2-1* and an *ltp1 ltp2* double knockdown; all seedlings were grown in the dark for 7 d after stratification on MS + 1% sucrose. Within each box, horizontal lines represent median values; boxes extend from the 25th to 75th percentiles; vertical lines denote adjacent values within 1.5 interquartile ranges; circles are observations outside of these ranges. (h) Representative images of toluidine blue stained etiolated hypocotyls from Col-0, *ltp2-1* and an *ltp1 ltp2* double mutant grown for 7 d after stratification on MS + 1% sucrose.

the short sample comparison (996/1164, 86%) did not overlap with the DEGs in the long sample comparison. Because the *ltp2* seedlings with long hypocotyls and Col-0 wild-type seedlings with long hypocotyls differ in genotype but little in mean hypocotyl length, we conclude that the gene expression differences across samples are strongly associated with hypocotyl length, in particular with the strongly reduced hypocotyl length of short *ltp2* seedlings.

ltp2 phenotypes depend on upregulation of its closest paralog *LTP1*

Focusing on cuticle-related genes (see methods from Li-Beisson *et al.*, 2013), we found that 21 out of the 160 expressed in dark-grown shoots were deregulated in *ltp2* relative to Col-0 seedlings (30% more than expected, $P = 0.019$; Table S6). Most of these genes (19/21) were upregulated in *ltp2*, including six other LTP paralogs (Fig. 4a). To explore to what extent close paralogs may compensate for reduced *LTP2* expression, we examined the role of its nearest paralog, *LTP1* (Figs 4b, S7A). Analysis of *LTP1* and *LTP2* expression in light- and dark-grown wild-type seedlings showed a reciprocal expression pattern that suggests nonredundant roles during hypocotyl elongation: Whereas *LTP1* was *c.* 100 times more abundant than *LTP2* in the light, it was 1/10 times as abundant in the dark (Fig. 4c). In dark-grown seedlings, *LTP2* accounts for > 86% of global Type I LTP expression compared with only 5% for *LTP1* (Fig. S7B). By stark contrast, *LTP1* tends to be the more abundantly expressed paralog in many other conditions, organs and developmental stages (41/56 samples; Fig. S7C). Moreover, we found that *LTP1* expression was no longer repressed in the dark in *ltp2* seedlings (Figs 4C, S7B). To rule out that this trend was an artifact of bulk expression analysis, we measured *LTP1* and *LTP2* expression in individual wild-type Col-0 and *ltp2-1* seedlings and measured the length of their hypocotyls. *LTP1* expression levels in individual *ltp2-1* seedlings recapitulated our bulk observations, and their hypocotyl lengths were negatively correlated with *LTP1* expression (Fig. S8; Spearman rho = −0.401; $P = 0.0108$). We further found that *LTP1* and *LTP2* expression levels were correlated across individual seedlings in both wild-type and *ltp2-1* seedlings (Fig. S8A; Col-0: 0.832; $P < 2.2e\text{-}16$; *ltp2-1*: 0.933; $P < 2.2e\text{-}16$), suggesting that the *LTP1*/*LTP2* expression ratio may matter for phenotype. Indeed, we observed that *LTP1*/*LTP2* expression ratios were weakly but significantly

correlated with hypocotyl length across individual *ltp2-1* and wild-type seedlings (Fig. S8E; Spearman's rho = 0.484, $P = 0.0018$ *ltp2-1*; Spearman's rho = 0.437, $P = 0.0059$ Col-0).

We next tested whether the altered expression ratio of the paralogs might contribute to the *ltp2* phenotypes in transgenic lines. We used an artificial microRNA to simultaneously knockdown *LTP1* and *LTP2* gene expression while aiming for a similar *LTP1*/*LTP2* ratio as found in Col-0 wild-type (Fig. 4d). Indeed, the mean value and variation of hypocotyl length of the *ltp1 ltp2* double knock-down seedlings closely resembled those of Col-0 wild-type seedlings with both distributions largely overlapping (Fig. 4e, f). The *ltp1 ltp2* double knock-down seedlings were also similar to Col-0 wild-type seedlings in hypocotyl : root ratio (Fig. 4g) and hypocotyl cuticle integrity (Fig. 4h). This result is even more remarkable considering that the expression levels of the individual *LTP1* and *LTP2* genes differed substantially in the *ltp1 ltp2* double knock-down seedlings from those observed in wild-type Col-0 seedlings (Fig. S9), consistent with their expression ratio as a determinant of the hypomorph phenotype. We conclude that the upregulation of *LTP1* compared with low expression levels of *LTP2* in dark-grown seedlings contributes to the variable skotomorphogenesis phenotypes of the *ltp2* hypomorphs.

Discussion

Here, we show that the gene *LTP2* plays an important role in shaping skotomorphogenesis traits. Hypomorphs of *LTP2* show increased phenotypic variation in three hypocotyl traits: negative gravitropism, length and cuticle permeability. For the latter two, the increased variation was accompanied by altered mean values relative to wild-type, with most *ltp2* dark-grown seedlings having short hypocotyls with highly permeable cuticles. Variation in hypocotyl length increases in dark-grown hypocotyls upon perturbation of the chaperone Hsp90 (Queitsch *et al.*, 2002; Sangster *et al.*, 2008), or its client protein BEH4 (Lachowiec *et al.*, 2018), as well as in *AGO1* hypomorphs (Lemus *et al.*, 2023). As for the *ltp2* hypomorphs described here, in these three cases, the increased variation in hypocotyl length was also accompanied by decreased length means. This concordance of changes in mean and variation might be expected if wild-type hypocotyls reach lengths close to their maximum physiological limit under these experimental conditions.

In *ltp2* hypocotyls, a strong defect in cuticle permeability was associated with reduced elongation and increased phenotypic variation compared with wild-type; however, these phenotypes depended on exposure to sucrose. This remarkably strong gene-by-environment effect is unlikely due to a higher requirement for LTP2 function, as hypocotyls elongate more when provided with an exogenous carbon source. *LIPID TRANSFER PROTEIN 2* is required in dark-grown hypocotyls to seal the cuticle and prevent water loss (Jacq *et al.*, 2017). Moreover, increased cuticle permeability is linked to structural defects and poor adhesion between the cuticle and the rest of the cell wall. Our finding that *ltp2* hypocotyls were much more susceptible to sucrose-induced dye uptake than wild-type is consistent with *LTP2*'s role in cuticle sealing and suggests that sucrose acts as a cuticle stress. Sucrose may trigger gene expression changes that modify cuticle composition or act directly to increase cuticle hydration, the mechanical strain associated with water accumulating in the cuticle and in gaps between the cuticle and the cell wall. This added strain could lead to further cuticle detachment in sensitized *ltp2* hypocotyls, thus aggravating their documented cuticle integrity defect (Jacq *et al.*, 2017). The sucrose-induced loss of cuticle integrity is likely the primary determinant of the shorter *ltp2* hypocotyls and their increased variation in length.

Dark-grown long hypocotyls have thick cuticles (Gendreau *et al.*, 1997), and shorter hypocotyls are associated with pharmacological or genetic disruptions in cuticular wax biosynthesis and deposition (Narukawa *et al.*, 2015). The greater need for cuticle integrity during hypocotyl elongation in the dark may reflect a seedling's push upwards through the soil while minimizing abrasion and the need for structural reinforcement due to cell wall thinning in very long cells (Derbyshire *et al.*, 2007). Loss of cuticle barrier function causes water loss and activates cuticle-dependent defense priming (Bessire *et al.*, 2007; Chassot *et al.*, 2007; L'Haridon *et al.*, 2011; Serrano *et al.*, 2014), which inhibits growth, and is consistent with the GO enrichments observed among upregulated genes in *ltp2* seedlings with short hypocotyls compared with those with long ones. However, the precise mechanisms by which *LPT2* facilitates the elongation of dark-grown hypocotyls remain unknown.

In contrast to phenotypic buffers, which act on gene regulation (Lachowiec *et al.*, 2016, 2018; Lemus *et al.*, 2023) or protein folding (Queitsch *et al.*, 2002; Sangster *et al.*, 2008; Lachowiec *et al.*, 2016; Zabinsky *et al.*, 2019), *LTP2* appears to act structurally by sealing the cuticle. The integrity of this seal determines the effectiveness of the cuticle as an insulating barrier, thus providing a simple mechanism of phenotypic robustness against environmental insults. Biophysical and regulatory complexity makes plant cuticles liable to harbor considerable nongenetic variation in their composition, ultra-structure and properties, in particular when considering the complexity of the environments plants face. Upon damage or genetic perturbation, this intrinsic variation is amplified as shown by the disorganized cuticles of mutants with cutin defects or increased cuticle permeability (Lolle *et al.*, 1992; Sieber *et al.*, 2000; Wellesen *et al.*, 2001; Chen *et al.*, 2003; Schnurr *et al.*, 2004; Kurdyukov *et al.*, 2006; Takahashi *et al.*, 2009).

Loss of cuticle integrity may not fully explain the increased phenotypic variation of *ltp2* seedlings. We cannot rule out that the increased phenotypic variation depends on another, yet undiscovered *LTP2*- function. However, our results that show genetic interaction between the close paralogs *LTP1* and *LTP2*, and that their expression ratio is a determinant of increased cuticle permeability and phenotypic variation during skotomorphogenesis, strongly support our interpretation. In crown gall tumors, the only other context outside of skotomorphogenesis where *ltp2* phenotypes have been identified (Jacq *et al.*, 2017), *LTP1* is also highly upregulated (Deeken *et al.*, 2016). This finding is consistent with our result that the upregulation of *LTP1* compared with *LTP2* expression is predictive of the deleterious *ltp2* phenotypes.

While paralogs with redundant or partially redundant functions can confer genetic robustness (Gu *et al.*, 2003; Kafri *et al.*, 2005; Dean *et al.*, 2008; DeLuna *et al.*, 2008, 2010; Diss *et al.*, 2013), this is not universally observed (Ihmels *et al.*, 2007; DeLuna *et al.*, 2010; Diss *et al.*, 2017; Dandage & Landry, 2019). In fact, incomplete functional compensation can be a source of increased phenotypic variation (Burga *et al.*, 2011; Bauer *et al.*, 2015). For example, *BEH4*, the earliest diverged member of the *BZR/BEH* family of transcription factors, governs phenotypic robustness of hypocotyl length by integrating regulatory cross-talk among the six gene family members (Lachowiec *et al.*, 2018). Thus, even among these closely related, partially redundant paralogs, increased trait variation arises when the activity of *BEH4* is lost. The loss of properly integrated regulatory cross-talk as a cause of increased phenotypic variation is consistent with our findings that upregulation of *LTP1* in the dark is associated with the *ltp2* phenotypes.

Subtle changes in gene expression that percolate through gene regulatory networks and amplify each other to affect expression of certain core genes are thought to underlie complex diseases and complex traits in humans (the omnigenic model; Boyle *et al.*, 2017; Liu *et al.*, 2019). The genetic variants found to be associated with complex diseases and traits in genome-wide association studies (GWAS) typically reside in regulatory regions, likely resulting in hypomorphs. The trait heritability explained by GWAS variants tends to be small, and these variants have little power to predict the disease risk of individuals (Manolio *et al.*, 2009; Eichler *et al.*, 2010; Gibson, 2012; Khera *et al.*, 2018). The low power to predict phenotype from genotype is consistent with high nongenetic trait variation (Queitsch *et al.*, 2012). We speculate that this nongenetic variation arises because regulatory variants cause small expression changes that are integrated differently among individuals. In turn, these differences in integrating expression changes will sensitize certain individuals but not others to environmental factors, resulting in different phenotypes. At least for *LTP2*, this interpretation holds: the upregulation of *LTP1* is not sufficient for the observed phenotypes as all *ltp2* seedlings exhibit it. Likewise, all *ltp2* seedlings experience exposure to sucrose; however, not all seedlings have short hypocotyls and show loss of cuticle integrity. The loss of barrier (i.e. cuticle) function in this plant example likely holds lessons for studies of human traits and diseases and points to genotype-by-environment effects as a major contributor to nongenetic variation.

Our study highlights that even highly inbred, *de facto* homozygous genetic backgrounds maintain a physiologically relevant reservoir of phenotypic variation, which can be exposed by stress. While stress often increases phenotypic variation in isogenic and inbred populations (Thattai & van Oudenaarden, 2004; Newman *et al.*, 2006; Braendle & Félix, 2008; Tokatlidis *et al.*, 2010; Uyttewaal *et al.*, 2012; Holland *et al.*, 2013; Mitosch *et al.*, 2017; Sandner *et al.*, 2021; de Groot *et al.*, 2023), phenotypic robustness (i.e. low nongenetic variation) is associated with stress tolerance and vigor in crops and lifestock (Tollenaar & Lee, 2002; Blasco *et al.*, 2017; Elgersma *et al.*, 2018). A common strategy to achieve phenotypic robustness coupled with high performance in agricultural settings has been the use of F1 hybrids, which are often more uniform in phenotype than their inbred parental lines (Lewis, 1953; Smith *et al.*, 1995; Phelan & Austad, 1994). A better understanding of the mechanistic underpinnings of nongenetic phenotypic variation might lead to the development of crops and livestock that combine uniformity of phenotype with broad stress tolerance. This better understanding of nongenetic phenotypic variation will also facilitate efforts to unravel the complexity of non-Mendelian human traits and diseases.

Acknowledgements

This work was supported by the National Science Foundation (NSF MCB-1242744, RESEARCH-PGR grant 1748843, PlantSynBio 2240888 to CQ) and the National Institute of Health (NIH NHGRI 5RM1HG010461, NIH NIGMS R35GM139532 to CQ).

Competing interests

None declared.

Author contributions

CMA, KMS and JL performed the experiments. CMA, KLB and JTC analyzed the data. CMA, KLB, JTC and CQ wrote the manuscript. All authors read and approved the final manuscript.

ORCID

Cristina M. Alexandre https://orcid.org/0000-0003-0047-0312
Kerry L. Bubb https://orcid.org/0000-0002-1117-2591
Josh T. Cuperus https://orcid.org/0000-0002-8019-7733
Christine Queitsch https://orcid.org/0000-0002-0905-4705

Data availability

RNA-Seq data are available at GEO (https://www.ncbi.nlm.nih.gov/geo/) BioProject ID PRJNA856271.

REFERENCES

Abley K, Formosa-Jordan P, Tavares H, Chan EY, Afsharinafar M, Leyser O, Locke JC. 2021. An ABA-GA bistable switch can account for natural variation in the variability of Arabidopsis seed germination time. *eLife* **10**: e59485.

Ansel J, Bottin H, Rodriguez-Beltran C, Damon C, Nagarajan M, Fehrmann S, François J, Yvert G. 2008. Cell-to-cell stochastic variation in gene expression is a complex genetic trait. *PLoS Genetics* **4**: e1000049.

Arondel VV, Vergnolle C, Cantrel C, Kader J. 2000. Lipid transfer proteins are encoded by a small multigene family in *Arabidopsis thaliana*. *Plant Science* **157**: 1–12.

Ayroles JF, Buchanan SM, O'Leary C, Skutt-Kakaria K, Grenier JK, Clark AG, Hartl DL, de Bivort BL. 2015. Behavioral idiosyncrasy reveals genetic control of phenotypic variability. *Proceedings of the National Academy of Sciences, USA* **112**: 6706–6711.

Bauer CR, Li S, Siegal ML. 2015. Essential gene disruptions reveal complex relationships between phenotypic robustness, pleiotropy, and fitness. *Molecular Systems Biology* **11**: 773.

Bessire M, Chassot C, Jacquat A-C, Humphry M, Borel S, Petétot JM-C, Métraux J-P, Nawrath C. 2007. A permeable cuticle in Arabidopsis leads to a strong resistance to *Botrytis cinerea*. *EMBO Journal* **26**: 2158–2168.

Blake WJ, Kaern M, Cantor CR, Collins JJ. 2003. Noise in eukaryotic gene expression. *Nature* **422**: 633–637.

Blasco A, Martínez-Álvaro M, García M-L, Ibáñez-Escriche N, Argente M-J. 2017. Selection for environmental variance of litter size in rabbits. *Genetics Selection Evolution* **49**: 48.

Bodenhofer U, Bonatesta E, Horejš-Kainrath C, Hochreiter S. 2015. msa: an R package for multiple sequence alignment. *Bioinformatics* **31**: 3997–3999.

Borevitz JO, Maloof JN, Lutes J, Dabi T, Redfern JL, Trainer GT, Werner JD, Asami T, Berry CC, Weigel D *et al.* 2002. Quantitative trait loci controlling light and hormone response in two accessions of *Arabidopsis thaliana*. *Genetics* **160**: 683–696.

Boyle EA, Li YI, Pritchard JK. 2017. An expanded view of complex traits: from polygenic to omnigenic. *Cell* **169**: 1177–1186.

Braendle C, Félix M-A. 2008. Plasticity and errors of a robust developmental system in different environments. *Developmental Cell* **15**: 714–724.

Bray NL, Pimentel H, Melsted P, Pachter L. 2016. Near-optimal probabilistic RNA-seq quantification. *Nature Biotechnology* **34**: 525–527.

Buhot N, Douliez JP, Jacquemard A, Marion D, Tran V, Maume BF, Milat ML, Ponchet M, Mikès V, Kader JC *et al.* 2001. A lipid transfer protein binds to a receptor involved in the control of plant defence responses. *FEBS Letters* **509**: 27–30.

Burga A, Casanueva MO, Lehner B. 2011. Predicting mutation outcome from early stochastic variation in genetic interaction partners. *Nature* **480**: 250–253.

Cameron KD, Moskal WA, Smart LB. 2006. A second member of the *Nicotiana glauca* lipid transfer protein gene family, NgLTP2, encodes a divergent and differentially expressed protein. *Functional Plant Biology* **33**: 141–152.

Casanueva MO, Burga A, Lehner B. 2012. Fitness trade-offs and environmentally induced mutation buffering in isogenic *C. elegans*. *Science* **335**: 82–85.

Chae K, Gonong BJ, Kim S-C, Kieslich CA, Morikis D, Balasubramanian S, Lord EM. 2010. A multifaceted study of stigma/style cysteine-rich adhesin (SCA)-like Arabidopsis lipid transfer proteins (LTPs) suggests diversified roles for these LTPs in plant growth and reproduction. *Journal of Experimental Botany* **61**: 4277–4290.

Chae K, Kieslich CA, Morikis D, Kim S-C, Lord EM. 2009. A gain-of-function mutation of Arabidopsis lipid transfer protein 5 disturbs pollen tube tip growth and fertilization. *Plant Cell* **21**: 3902–3914.

Chassot C, Nawrath C, Métraux J. 2007. Cuticular defects lead to full immunity to a major plant pathogen. *The Plant Journal* **49**: 972–980.

Chen X, Goodwin SM, Boroff VL, Liu X, Jenks MA. 2003. Cloning and characterization of the WAX2 gene of Arabidopsis involved in cuticle membrane and wax production. *Plant Cell* **15**: 1170–1185.

Dandage R, Landry CR. 2019. Paralog dependency indirectly affects the robustness of human cells. *Molecular Systems Biology* **15**: e8871.

Dean EJ, Davis JC, Davis RW, Petrov DA. 2008. Pervasive and persistent redundancy among duplicated genes in yeast. *PLoS Genetics* **4**: e1000113.

Debono A, Yeats TH, Rose JKC, Bird D, Jetter R, Kunst L, Samuels L. 2009. Arabidopsis LTPG is a glycosylphosphatidylinositol-anchored lipid transfer protein required for export of lipids to the plant surface. *Plant Cell* **21**: 1230–1238.

Deeken R, Saupe S, Klinkenberg J, Riedel M, Leide J, Hedrich R, Mueller TD. 2016. The nonspecific lipid transfer protein AtLtpI-4 is involved in suberin formation of *Arabidopsis thaliana* crown galls. *Plant Physiology* **172**: 1911–1927.

DeLuna A, Springer M, Kirschner MW, Kishony R. 2010. Need-based up-regulation of protein levels in response to deletion of their duplicate genes. *PLoS Biology* **8**: e1000347.

DeLuna A, Vetsigian K, Shoresh N, Hegreness M, Colón-González M, Chao S, Kishony R. 2008. Exposing the fitness contribution of duplicated genes. *Nature Genetics* **40**: 676–681.

Delvigne F, Goffin P. 2014. Microbial heterogeneity affects bioprocess robustness: dynamic single-cell analysis contributes to understanding of microbial populations. *Biotechnology Journal* **9**: 61–72.

Derbyshire P, McCann MC, Roberts K. 2007. Restricted cell elongation in Arabidopsis hypocotyls is associated with a reduced average pectin esterification level. *BMC Plant Biology* **7**: 31.

Diss G, Ascencio D, DeLuna A, Landry CR. 2013. Molecular mechanisms of paralogous compensation and the robustness of cellular networks. *Journal of Experimental Zoology Part B: Molecular and Developmental Evolution* **322**: 488–499.

Diss G, Gagnon-Arsenault I, Dion-Coté A-M, Vignaud H, Ascencio DI, Berger CM, Landry CR. 2017. Gene duplication can impart fragility, not robustness, in the yeast protein interaction network. *Science* **355**: 630–634.

Eagle H, Levine EM. 1967. Growth regulatory effects of cellular interaction. *Nature* **213**: 1102–1106.

Eichler EE, Flint J, Gibson G, Kong A, Leal SM, Moore JH, Nadeau JH. 2010. Missing heritability and strategies for finding the underlying causes of complex disease. *Nature Reviews Genetics* **11**: 446–450.

Eldar A, Chary VK, Xenopoulos P, Fontes ME, Losón OC, Dworkin J, Piggot PJ, Elowitz MB. 2009. Partial penetrance facilitates developmental evolution in bacteria. *Nature* **460**: 510–514.

Elgersma GG, de Jong G, van der Linde R, Mulder HA. 2018. Fluctuations in milk yield are heritable and can be used as a resilience indicator to breed healthy cows. *Journal of Dairy Science* **101**: 1240–1250.

Elowitz MB, Levine AJ, Siggia ED, Swain PS. 2002. Stochastic gene expression in a single cell. *Science* **297**: 1183–1186.

Emert BL, Cote CJ, Torre EA, Dardani IP, Jiang CL, Jain N, Shaffer SM, Raj A. 2021. Variability within rare cell states enables multiple paths toward drug resistance. *Nature Biotechnology* **39**: 865–876.

Feinerman O, Veiga J, Dorfman JR, Germain RN, Altan-Bonnet G. 2008. Variability and robustness in T cell activation from regulated heterogeneity in protein levels. *Science* **321**: 1081–1084.

Finch-Savage WE, Bassel GW. 2016. Seed vigour and crop establishment: extending performance beyond adaptation. *Journal of Experimental Botany* **67**: 567–591.

Finkina EI, Melnikova DN, Bogdanov IV, Ovchinnikova TV. 2016. Lipid transfer proteins as components of the plant innate immune system: structure, functions, and applications. *Acta Naturae* **8**: 47–61.

Gao S, Guo W, Feng W, Liu L, Song X, Chen J, Hou W, Zhu H, Tang S, Hu J. 2016. LTP3 contributes to disease susceptibility in Arabidopsis by enhancing abscisic acid (ABA) biosynthesis. *Molecular Plant Pathology* **17**: 412–426.

Geldner N. 2013. The endodermis. *Annual Review of Plant Biology* **64**: 531–558.

Gendreau E, Traas J, Desnos T, Grandjean O, Caboche M, Höfte H. 1997. Cellular basis of hypocotyl growth in *Arabidopsis thaliana*. *Plant Physiology* **114**: 295–305.

Gibson G. 2012. Rare and common variants: twenty arguments. *Nature Reviews Genetics* **13**: 135–145.

Gimelbrant A, Hutchinson JN, Thompson BR, Chess A. 2007. Widespread monoallelic expression on human autosomes. *Science* **318**: 1136–1140.

de Groot DH, Tjalma AJ, Bruggeman FJ, van Nimwegen E. 2023. Effective bet-hedging through growth rate dependent stability. *Proceedings of the National Academy of Sciences, USA* **120**: e2211091120.

Gu Z, Steinmetz LM, Gu X, Scharfe C, Davis RW, Li W-H. 2003. Role of duplicate genes in genetic robustness against null mutations. *Nature* **421**: 63–66.

Hall MC, Dworkin I, Ungerer MC, Purugganan M. 2007. Genetics of microenvironmental canalization in *Arabidopsis thaliana*. *Proceedings of the National Academy of Sciences, USA* **104**: 13717–13722.

Hartwell LH, Culotti J, Pringle JR, Reid BJ. 1974. Genetic control of the cell division cycle in yeast. *Science* **183**: 46–51.

Heerden JHV, Wortel MT, Bruggeman FJ, Heijnen JJ, Bollen YJ, Planqué R, Hulshof J, O'Toole TG, Wahl SA, Teusink B. 2014. Fatal attraction in glycolysis: how *Saccharomyces cerevisiae* manages sudden transitions to high glucose. *Microbial Cell* **1**: 103–106.

Hill WG, Mulder HA, Zhang X-S. 2007. The quantitative genetics of phenotypic variation in animals. *Acta Agriculturae Scandinavica, Section A – Animal Science* **57**: 175–182.

Holland SL, Reader T, Dyer PS, Avery SV. 2013. Phenotypic heterogeneity is a selected trait in natural yeast populations subject to environmental stress. *Environmental Microbiology* **16**: 1729–1740.

Hong L, Dumond M, Tsugawa S, Sapala A, Routier-Kierzkowska A-L, Zhou Y, Chen C, Kiss A, Zhu M, Hamant O *et al.* 2016. Variable cell growth yields reproducible organ development through spatiotemporal averaging. *Developmental Cell* **38**: 15–32.

Ihmels J, Collins SR, Schuldiner M, Krogan NJ, Weissman JS. 2007. Backup without redundancy: genetic interactions reveal the cost of duplicate gene loss. *Molecular Systems Biology* **3**: 86.

Illouz-Eliaz N, Ramon U, Shohat H, Blum S, Livne S, Mendelson D, Weiss D. 2019. Multiple gibberellin receptors contribute to phenotypic stability under changing environments. *Plant Cell* **31**: 1506–1519.

Irshad M, Canut H, Borderies G, Pont-Lezica R, Jamet E. 2008. A new picture of cell wall protein dynamics in elongating cells of *Arabidopsis thaliana*: confirmed actors and newcomers. *BMC Plant Biology* **8**: 94.

Jacq A, Pernot C, Martinez Y, Domergue F, Payré B, Jamet E, Burlat V, Pacquit VB. 2017. The Arabidopsis lipid transfer protein 2 (AtLTP2) is involved in cuticle-cell wall interface integrity and in etiolated hypocotyl permeability. *Frontiers in Plant Science* **8**: 263.

Jimenez-Gomez JM, Corwin JA, Joseph B, Maloof JN, Kliebenstein DJ. 2011. Genomic analysis of QTLs and genes altering natural variation in stochastic noise. *PLoS Genetics* **7**: e1002295.

Joseph B, Corwin JA, Kliebenstein DJ. 2015. Genetic variation in the nuclear and organellar genomes modulates stochastic variation in the metabolome, growth, and defense. *PLoS Genetics* **11**: e1004779.

Kader J-C. 1996. Lipid-transfer proteins in plants. *Annual Review of Plant Physiology and Plant Molecular Biology* **47**: 627–654.

Kafri R, Bar-Even A, Pilpel Y. 2005. Transcription control reprogramming in genetic backup circuits. *Nature Genetics* **37**: 295–299.

Kalve S, Sizani BL, Markakis MN, Helsmoortel C, Vandeweyer G, Laukens K, Sommen M, Naulaerts S, Vissenberg K, Prinsen E *et al.* 2020. Osmotic stress inhibits leaf growth of *Arabidopsis thaliana* by enhancing ARF-mediated auxin responses. *New Phytologist* **226**: 1766–1780.

Kanno T, Mette MF, Kreil DP, Aufsatz W, Matzke M, Matzke AJM. 2004. Involvement of putative SNF2 chromatin remodeling protein DRD1 in RNA-directed DNA methylation. *Current Biology* **14**: 801–805.

Karahara I. 2012. The pea stem: a unique experimental system to study the development of the Casparian strip. *Plant Signaling & Behavior* **7**: 1182–1184.

Katsanos D, Koneru SL, Mestek Boukhibar L, Gritti N, Ghose R, Appleford PJ, Doitsidou M, Woollard A, van Zon JS, Poole RJ *et al.* 2017. Stochastic loss and gain of symmetric divisions in the *C. elegans* epidermis perturbs robustness of stem cell number. *PLoS Biology* **15**: e2002429.

Khera AV, Chaffin M, Aragam KG, Haas ME, Roselli C, Choi SH, Natarajan P, Lander ES, Lubitz SA, Ellinor PT *et al.* 2018. Genome-wide polygenic scores for common diseases identify individuals with risk equivalent to monogenic mutations. *Nature Genetics* **50**: 1219–1224.

Kircher S, Schopfer P. 2012. Photosynthetic sucrose acts as cotyledon-derived long-distance signal to control root growth during early seedling development in Arabidopsis. *Proceedings of the National Academy of Sciences, USA* **109**: 11217–11221.

Kurdyukov S, Faust A, Nawrath C, Bär S, Efremova N, Voisin D, Efremova N, Franke R, Schreiber L, Saedler H *et al.* 2006. The epidermis-specific extracellular BODYGUARD controls cuticle development and morphogenesis in Arabidopsis. *Plant Cell* **18**: 321–339.

L'Haridon F, Besson-Bard A, Binda M, Serrano M, Abou-Mansour E, Balet F, Schoonbeek H-J, Hess S, Mir R, Léon J *et al.* 2011. A permeable cuticle is associated with the release of reactive oxygen species and induction of innate immunity. *PLoS Pathogens* **7**: e1002148.

Lachowiec J, Mason GA, Schultz K, Queitsch C. 2018. Redundancy, feedback, and robustness in the *Arabidopsis thaliana* BZR/BEH gene family. *Frontiers in Genetics* **9**: 523.

Lachowiec J, Queitsch C, Kliebenstein DJ. 2016. Molecular mechanisms governing differential robustness of development and environmental responses in plants. *Annals of Botany* **117**: 795–809.

Lemus T, Mason GA, Bubb KL, Alexandre CM, Queitsch C, Cuperus JT. 2023. AGO1 and HSP90 buffer different genetic variants in *Arabidopsis thaliana*. *Genetics* **223**: iyac163.

Lewis D. 1953. A relationship between dominance, phenotypic stability and variability, and a theory of alternative genetic pathways. *Nature* **172**: 1136–1137.

Li-Beisson Y, Shorrosh B, Beisson F, Andersson MX, Arondel V, Bates PD, Baud S, Bird D, DeBono A, Durrett TP *et al.* 2013. Acyl-lipid metabolism. *The Arabidopsis Book* **11**: e0161.

Liu X, Li YI, Pritchard JK. 2019. Trans effects on gene expression can drive omnigenic inheritance. *Cell* **177**: 1022–1034.

Lolle SJ, Cheung AY, Sussex IM. 1992. Fiddlehead: an Arabidopsis mutant constitutively expressing an organ fusion program that involves interactions between epidermal cells. *Developmental Biology* **152**: 383–392.

Lomvardas S, Barnea G, Pisapia DJ, Mendelsohn M, Kirkland J, Axel R. 2006. Interchromosomal interactions and olfactory receptor choice. *Cell* **126**: 403–413.

Love MI, Huber W, Anders S. 2014. Moderated estimation of fold change and dispersion for RNA-seq data with DESeq2. *Genome Biology* **15**: 550.

Maldonado AM, Doerner P, Dixon RA, Lamb CJ, Cameron RK. 2002. A putative lipid transfer protein involved in systemic resistance signalling in Arabidopsis. *Nature* **419**: 399–403.

Maloof JN, Borevitz JO, Dabi T, Lutes J, Nehring RB, Redfern JL, Trainer GT, Wilson JM, Asami T, Berry CC *et al.* 2001. Natural variation in light sensitivity of Arabidopsis. *Nature Genetics* **29**: 441–446.

Manolio TA, Collins FS, Cox NJ, Goldstein DB, Hindorff LA, Hunter DJ, McCarthy MI, Ramos EM, Cardon LR, Chakravarti A *et al.* 2009. Finding the missing heritability of complex diseases. *Nature* **461**: 747–753.

Márquez-Jurado S, Díaz-Colunga J, Das Neves RP, Martinez-Lorente A, Almazán F, Guantes R, Iborra FJ. 2018. Mitochondrial levels determine variability in cell death by modulating apoptotic gene expression. *Nature Communications* **9**: 389.

Mason GA, Lemus T, Queitsch C. 2016. The mechanistic underpinnings of an ago1-mediated, environmentally dependent, and stochastic phenotype. *Plant Physiology* **170**: 2420–2431.

Miedes E, Suslov D, Vandenbussche F, Kenobi K, Ivakov A, Van Der Straeten D, Lorences EP, Mellerowicz EJ, Verbelen J-P, Vissenberg K. 2013. Xyloglucan endotransglucosylase/hydrolase (XTH) overexpression affects growth and cell wall mechanics in etiolated Arabidopsis hypocotyls. *Journal of Experimental Botany* **64**: 2481–2497.

Mitosch K, Rieckh G, Bollenbach T. 2017. Noisy response to antibiotic stress predicts subsequent single-cell survival in an acidic environment. *Cell Systems* **4**: 393–403.

Molina A, García-Olmedo F. 1993. Developmental and pathogen-induced expression of three barley genes encoding lipid transfer proteins. *The Plant Journal* **4**: 983–991.

Narukawa H, Yokoyama R, Nishitani K. 2015. Possible pathways linking ploidy level to cell elongation and cuticular function in hypocotyls of dark-grown Arabidopsis seedlings. *Plant Signaling & Behavior* **11**: e1118597.

Newman JRS, Ghaemmaghami S, Ihmels J, Breslow DK, Noble M, DeRisi JL, Weissman JS. 2006. Single-cell proteomic analysis of *S. cerevisiae* reveals the architecture of biological noise. *Nature* **441**: 840–846.

Nieuwland J, Feron R, Huisman BAH, Fasolino A, Hilbers CW, Derksen J, Mariani C. 2005. Lipid transfer proteins enhance cell wall extension in tobacco. *Plant Cell* **17**: 2009–2019.

Paradis E, Claude J, Strimmer K. 2004. APE: analyses of phylogenetics and evolution in R language. *Bioinformatics* **20**: 289–290.

Park J-E, Kim Y-S, Yoon H-K, Park C-M. 2007. Functional characterization of a small auxin-up RNA gene in apical hook development in Arabidopsis. *Plant Science* **172**: 150–157.

Perez MF, Francesconi M, Hidalgo-Carcedo C, Lehner B. 2017. Maternal age generates phenotypic variation in *Caenorhabditis elegans*. *Nature* **552**: 106–109.

Phelan JP, Austad SN. 1994. Selecting animal models of human aging: inbred strains often exhibit less biological uniformity than F1 hybrids. *Journal of Gerontology* **49**: B1–B11.

Potocka I, Baldwin TC, Kurczynska EU. 2012. Distribution of lipid transfer protein 1 (LTP1) epitopes associated with morphogenic events during somatic embryogenesis of *Arabidopsis thaliana*. *Plant Cell Reports* **31**: 2031–2045.

Queitsch C, Carlson KD, Girirajan S. 2012. Lessons from model organisms: phenotypic robustness and missing heritability in complex disease. *PLoS Genetics* **8**: e1003041.

Queitsch C, Sangster TA, Lindquist S. 2002. Hsp90 as a capacitor of phenotypic variation. *Nature* **417**: 618–624.

Rai MI, Wang X, Thibault DM, Kim HJ, Bombyk MM, Binder BM, Shakeel SN, Schaller GE. 2015. The ARGOS gene family functions in a negative feedback loop to desensitize plants to ethylene. *BMC Plant Biology* **15**: 157.

Raj A, Rifkin SA, Andersen E, van Oudenaarden A. 2010. Variability in gene expression underlies incomplete penetrance. *Nature* **463**: 913–918.

Raser JM, O'Shea EK. 2004. Control of stochasticity in eukaryotic gene expression. *Science* **304**: 1811–1814.

Raudvere U, Kolberg L, Kuzmin I, Arak T, Adler P, Peterson H, Vilo J. 2019. g:Profiler: a web server for functional enrichment analysis and conversions of gene lists (2019 update). *Nucleic Acids Research* **47**: W191–W198.

Reed JW, Elumalai RP, Chory J. 1998. Suppressors of an *Arabidopsis thaliana* phyB mutation identify genes that control light signaling and hypocotyl elongation. *Genetics* **148**: 1295–1310.

Ros M, Sorensen D, Waagepetersen R, Dupont-Nivet M, SanCristobal M, Bonnet J-C, Mallard J. 2004. Evidence for genetic control of adult weight plasticity in the snail *Helix aspersa*. *Genetics* **168**: 2089–2097.

Sandner TM, Matthies D, Waller DM. 2021. Stresses affect inbreeding depression in complex ways: disentangling stress-specific genetic effects from effects of initial size in plants. *Heredity* **127**: 347–356.

Sangster TA, Salathia N, Lee HN, Watanabe E, Schellenberg K, Morneau K, Wang H, Undurraga S, Queitsch C, Lindquist S. 2008. HSP90-buffered genetic variation is common in *Arabidopsis thaliana*. *Proceedings of the National Academy of Sciences, USA* **105**: 2969–2974.

Sawa S, Ohgishi M, Goda H, Higuchi K, Shimada Y, Yoshida S, Koshiba T. 2002. The HAT2 gene, a member of the HD-Zip gene family, isolated as an auxin inducible gene by DNA microarray screening, affects auxin response in Arabidopsis. *The Plant Journal* **32**: 1011–1022.

Schnurr J, Shockey J, Browse J. 2004. The acyl-CoA synthetase encoded by LACS2 is essential for normal cuticle development in Arabidopsis. *Plant Cell* **16**: 629–642.

Serrano M, Coluccia F, Torres M, L'Haridon F, Métraux J-P. 2014. The cuticle and plant defense to pathogens. *Frontiers in Plant Science* **5**: 274.

Shaffer SM, Dunagin MC, Torborg SR, Torre EA, Emert B, Krepler C, Beqiri M, Sproesser K, Brafford PA, Xiao M *et al.* 2017. Rare cell variability and drug-induced reprogramming as a mode of cancer drug resistance. *Nature* **546**: 431–435.

Sharma SV, Lee DY, Li B, Quinlan MP, Takahashi F, Maheswaran S, McDermott U, Azizian N, Zou L, Fischbach MA *et al.* 2010. A chromatin-mediated reversible drug-tolerant state in cancer cell subpopulations. *Cell* **141**: 69–80.

Shen X, Pettersson M, Rönnegård L, Carlborg Ö. 2012. Inheritance beyond plain heritability: variance-controlling genes in *Arabidopsis thaliana*. *PLoS Genetics* **8**: e1002839.

Sieber P, Schorderet M, Ryser U, Buchala A, Kolattukudy P, Métraux J-P, Nawrath C. 2000. Transgenic Arabidopsis plants expressing a fungal cutinase show alterations in the structure and properties of the cuticle and postgenital organ fusions. *Plant Cell* **12**: 721–737.

Smith MCA, Sumner ER, Avery SV. 2007. Glutathione and Gts1p drive beneficial variability in the cadmium resistances of individual yeast cells. *Molecular Microbiology* **66**: 699–712.

Smith JM, Clarke JM, Hollingsworth MJ. 1995. The expression of hybrid vigour in *Drosophila subobscura*. *Proceedings of the Royal Society of London. Series B: Biological Sciences* **144**: 159–171.

Snijder B, Sacher R, Rämö P, Damm E-M, Liberali P, Pelkmans L. 2009. Population context determines cell-to-cell variability in endocytosis and virus infection. *Nature* **461**: 520–523.

Spartz AK, Lee SH, Wenger JP, Gonzalez N, Itoh H, Inzé D, Peer WA, Murphy AS, Overvoorde PJ, Gray WM. 2012. The SAUR19 subfamily of SMALL AUXIN UP RNA genes promote cell expansion. *The Plant Journal* **70**: 978–990.

Takahashi K, Shimada T, Kondo M, Tamai A, Mori M, Nishimura M, Hara-Nishimura I. 2009. Ectopic expression of an esterase, which is a candidate for the unidentified plant cutinase, causes cuticular defects in *Arabidopsis thaliana*. *Plant and Cell Physiology* **51**: 123–131.

Tanaka T, Tanaka H, Machida C, Watanabe M, Machida Y. 2004. A new method for rapid visualization of defects in leaf cuticle reveals five intrinsic patterns of surface defects in Arabidopsis. *The Plant Journal* **37**: 139–146.

Thattai M, van Oudenaarden A. 2004. Stochastic gene expression in fluctuating environments. *Genetics* **167**: 523–530.

Tian Q, Uhlir NJ, Reed JW. 2002. Arabidopsis SHY2/IAA3 inhibits auxin-regulated gene expression. *Plant Cell* **14**: 301–319.

Tokatlidis IS, Haş V, Mylonas I, Haş I, Evgenidis G, Melidis V, Copandean A, Ninou E. 2010. Density effects on environmental variance and expected response to selection in maize (*Zea mays* L.). *Euphytica* **174**: 283–291.

Tollenaar M, Lee EA. 2002. Yield potential, yield stability and stress tolerance in maize. *Field Crops Research* **75**: 161–169.

Tran DT, Hertog MLATM, Tran TLH, Quyen NT, Van de Poel B, Mata CI, Nicolaï BM. 2017. Population modeling approach to optimize crop harvest strategy. The case of field tomato. *Frontiers in Plant Science* **8**: 608.

Uyttewaal M, Burian A, Alim K, Landrein B, Borowska-Wykręt D, Dedieu A, Peaucelle A, Ludynia M, Traas J, Boudaoud A *et al.* 2012. Mechanical stress acts via katanin to amplify differences in growth rate between adjacent cells in Arabidopsis. *Cell* **149**: 439–451.

Vandenbussche F, Verbelen J-P, Van Der Straeten D. 2005. Of light and length: regulation of hypocotyl growth in Arabidopsis. *BioEssays: News and Reviews in Molecular, Cellular and Developmental Biology* **27**: 275–284.

Volfson D, Marciniak J, Blake WJ, Ostroff N, Tsimring LS, Hasty J. 2006. Origins of extrinsic variability in eukaryotic gene expression. *Nature* **439**: 861–864.

Waddington CH. 1942. Canalization of development and the inheritance of acquired characters. *Nature* **150**: 563–565.

Wellesen K, Durst F, Pinot F, Benveniste I, Nettesheim K, Wisman E, Steiner-Lange S, Saedler H, Yephremov A. 2001. Functional analysis of the LACERATA gene of Arabidopsis provides evidence for different roles of fatty acid ω-hydroxylation in development. *Proceedings of the National Academy of Sciences, USA* **98**: 9694–9699.

Whitlock MC, Fowler K. 1999. The changes in genetic and environmental variance with inbreeding in *Drosophila melanogaster*. *Genetics* **152**: 345–353.

Wright S. 1920. The relative importance of heredity and environment in determining the piebald pattern of Guinea-pigs. *Proceedings of the National Academy of Sciences, USA* **6**: 320–332.

Xiao C, Somerville C, Anderson CT. 2014. POLYGALACTURONASE INVOLVED IN EXPANSION1 functions in cell elongation and flower development in Arabidopsis. *Plant Cell* **26**: 1018–1035.

Xiao Y, Bowen CH, Liu D, Zhang F. 2016. Exploiting nongenetic cell-to-cell variation for enhanced biosynthesis. *Nature Chemical Biology* **12**: 339–344.

Yeats TH, Rose JKC. 2008. The biochemistry and biology of extracellular plant lipid-transfer proteins (LTPs). *Protein Science* **17**: 191–198.

Zabinsky RA, Mason GA, Queitsch C, Jarosz DF. 2019. It's not magic – Hsp90 and its effects on genetic and epigenetic variation. *Seminars in Cell & Developmental Biology* **88**: 21–35.

Ziemann M, Kaspi A, El-Osta A. 2019. Digital expression explorer 2: a repository of uniformly processed RNA sequencing data. *GigaScience* **8**: giz022.

Zwiewka M, Nodzyński T, Robert S, Vanneste S, Friml J. 2015. Osmotic stress modulates the balance between exocytosis and clathrin-mediated endocytosis in *Arabidopsis thaliana*. *Molecular Plant* **8**: 1175–1187.

Supporting Information

Additional Supporting Information may be found online in the Supporting Information section at the end of the article.

Fig. S1 *LTP2* expression is induced in the dark.

Fig. S2 Increased nongenetic variation in *ltp2* hypocotyl length is not explained by seed batch, germination time, or seed size.

Fig. S3 Exogenous sucrose modifies hypocotyl and root growth in etiolated seedlings.

Fig. S4 Mannitol improves hypocotyl elongation of sucrose-grown *ltp2* seedlings.

Fig. S5 *ltp2* hypocotyls show wild-type-like sucrose-induced responses.

Fig. S6 RNA-Seq on pools of long and short hypocotyls.

Fig. S7 Expression patterns of the close paralogs *LTP2* and *LTP1*.

Fig. S8 *LTP1* is upregulated across individual *ltp2-1* seedlings.

Fig. S9 *LTP1* and *LTP2* expression is low in *ltp1 ltp2* seedlings.

Table S1 List of primers used in genotyping and qRT-PCR.

Table S2 Differentially expressed genes between Col-L and Col-S.

Table S3 Differentially expressed genes between *ltp2*-L and *ltp2*-S.

Table S4 Differentially expressed genes between Col-L and *ltp2*-L.

Table S5 Differentially expressed genes between Col-S and *ltp2*-L.

Table S6 Cuticle-related genes expressed in our RNA-Seq dataset.

Table S7 List of publicly available RNA-Seq samples used to establish global expression patterns for *LTP1* and *LTP2*.

Table S8 Auxin-responsive DEGs, not shared between Col-S vs *ltp2*-S and *ltp2*-L vs *ltp2*-S.

Please note: Wiley is not responsible for the content or functionality of any Supporting Information supplied by the authors. Any queries (other than missing material) should be directed to the *New Phytologist* Central Office.